International Journal of
Molecular Sciences

MDPI

Article

Identification of Somatic Mutations in Plasma Cell-Free DNA from Patients with Metastatic Oral Squamous Cell Carcinoma

Li-Han Lin [1,†], Kuo-Wei Chang [2,3,†], Hui-Wen Cheng [1] and Chung-Ji Liu [1,2,4,*]

[1] Department of Medical Research, MacKay Memorial Hospital No. 92, Sec. 2, Chung San N. Rd., Taipei 10449, Taiwan
[2] Institute of Oral Biology, School of Dentistry, National Yang Ming Chiao Tung University, Taipei 11221, Taiwan
[3] Department of Stomatology, Taipei Veterans General Hospital, Taipei 11121, Taiwan
[4] Department of Oral and Maxillofacial Surgery, Taipei MacKay Memorial Hospital, Taipei 10449, Taiwan
* Correspondence: cjliu@mmh.org.tw; Fax: +886-25433642
† These authors contributed equally to this work.

Abstract: The accurate diagnosis and treatment of oral squamous cell carcinoma (OSCC) requires an understanding of its genomic alterations. Liquid biopsies, especially cell-free DNA (cfDNA) analysis, are a minimally invasive technique used for genomic profiling. We conducted comprehensive whole-exome sequencing (WES) of 50 paired OSCC cell-free plasma with whole blood samples using multiple mutation calling pipelines and filtering criteria. Integrative Genomics Viewer (IGV) was used to validate somatic mutations. Mutation burden and mutant genes were correlated to clinico-pathological parameters. The plasma mutation burden of cfDNA was significantly associated with clinical staging and distant metastasis status. The genes *TTN*, *PLEC*, *SYNE1*, and *USH2A* were most frequently mutated in OSCC, and known driver genes, including *KMT2D*, *LRP1B*, *TRRAP*, and *FLNA*, were also significantly and frequently mutated. Additionally, the novel mutated genes *CCDC168*, *HMCN2*, *STARD9*, and *CRAMP1* were significantly and frequently present in patients with OSCC. The mutated genes most frequently found in patients with metastatic OSCC were *RORC*, *SLC49A3*, and *NUMBL*. Further analysis revealed that branched-chain amino acid (BCAA) catabolism, extracellular matrix–receptor interaction, and the hypoxia-related pathway were associated with OSCC prognosis. Choline metabolism in cancer, O-glycan biosynthesis, and protein processing in the endoplasmic reticulum pathway were associated with distant metastatic status. About 20% of tumors carried at least one aberrant event in BCAA catabolism signaling that could possibly be targeted by an approved therapeutic agent. We identified molecular-level OSCC that were correlated with etiology and prognosis while defining the landscape of major altered events of the OSCC plasma genome. These findings will be useful in the design of clinical trials for targeted therapies and the stratification of patients with OSCC according to therapeutic efficacy.

Keywords: cell-free DNA; distant metastasis; liquid biopsy; mutation burden; oral cancer; whole-exome sequencing

Citation: Lin, L.-H.; Chang, K.-W.; Cheng, H.-W.; Liu, C.-J. Identification of Somatic Mutations in Plasma Cell-Free DNA from Patients with Metastatic Oral Squamous Cell Carcinoma. *Int. J. Mol. Sci.* **2023**, *24*, 10408. https://doi.org/10.3390/ijms241210408

Academic Editors: Shun-Fa Yang, Ana Caruntu and Julio Acero

Received: 8 May 2023
Revised: 1 June 2023
Accepted: 15 June 2023
Published: 20 June 2023

1. Introduction

Oral squamous cell carcinoma (OSCC) is a relatively common malignancy of the upper aerodigestive tract with poor prognosis and a high mortality rate. In Asia, 248,360 new OSCC cases (ICD10 C00-06—Lip, oral cavity) were diagnosed in 2020, among which 131,610 involved the death of the patient from the disease [1]. In about 4.0–7.4% of patients with OSCC, several tumors were found to be developing simultaneously in the head and neck region [2,3]. In addition to the high incidence and mortality rates worldwide [4], OSCC has a high recurrence rate after treatment, which may be because multiple lesions develop concurrently and over a large mucosal area [5]. To ensure the appropriate diagnosis and treatment of OSCC, the underlying genomic changes associated with the carcinogenesis of the disease must be understood.

Cell-free DNA (cfDNA) can originate from normal cells, including normal leukocytes undergoing apoptosis, or may be shed from dead normal cells or cancer cells. Thus, cfDNA is detectable in all patients, regardless of their health or cancer status [6–8]. Indeed, total cfDNA may consist of normal and tumor cfDNA in variable proportions [8]. For the diagnosis and surveillance of cancer, there is growing interest in plasma cfDNA, i.e., "liquid biopsy" [9–12]. cfDNA may originate from circulating tumor cells; therefore, the levels of cfDNA can reflect the presence of micrometastatic disease and the aggressiveness of the cancer [13]. Higher plasma cfDNA levels have been found in patients with oropharyngeal squamous cell carcinoma (OPSCC), a subtype of head and neck cancer, than in patients with other types of head and squamous cell carcinoma (HNSCC) [14]. For example, Lin et al. found 2.2-fold higher concentrations of cfDNA in patients with OSCC than in healthy controls [15].

Whole-exome sequencing (WES) has provided new insights into the molecular basis of OSCC progression [16–18]. Thus, WES analyses of cfDNA could lead to the discovery of novel resistance mechanisms, characterization of mutational signatures predicting treatment responses, identification of genes associated with disease progression, and/or capture of DNA signatures that aid treatment-associated decision-making [19–21]. To improve the diagnosis of individuals at risk and the treatment of OSCC, more sensitive and specific biomarkers are required [22,23]. Current evidence suggests that assessing cfDNA-derived somatic mutations in the plasma of OSCC patients according to a panel of genes could serve as a diagnostic or recurrence monitoring test [24–30].

Liebs et al. published the cfDNA mutation profiles of six metastasized HNSCC patients [30]. However, cfDNA has not been analyzed to determine the whole-exome somatic mutations in primary OSCC. Therefore, the aim of the present study was to obtain WES data from oral cancer cfDNA by sequencing 50 OSCC paired plasma/blood samples using a whole-exome platform. Somatic mutations were defined by referring to high-quality data obtained previously and using independent data and variant calling methods. The selected data were then combined and validated using the Integrative Genomics Viewer (IGV) to reduce false-positive calls but maintain the mutation detection sensitivity of the method. Finally, mutations identified as truly somatic were compared with clinical data.

2. Results

2.1. Characterization of Patients

In the paired analysis of the cfDNA and germline DNA of 50 OSCC patients, the fragment size distribution of cfDNA was ~150–200 bp (Supplementary Figure S1A), and cfDNA concentrations of 20–473 ng/mL were distributed in a wide range (Supplementary Figure S2A). Table 1 shows the clinical characteristics of the study subjects: 48 males and 2 females aged 40–89 years (mean age: 59.6 years). In Taiwan, the OSCC was male predominated and the male to female ratio was 16:1. Their primary lesions were most commonly located in the buccal region and the gingiva (28% and 24%, respectively).

Table 1. Association between plasma cfDNA mutation burden (PMB) and clinical parameters.

Parameter	N	Mean of PMB ± SD	*p*-Value
Age			
≤60	23	16.41 ± 26.43	0.661
>60	27	20.19 ± 31.78	
Gender			
Male	48	19.05 ± 29.67	0.766
Female	2	4.13 ± 1.68	
T stage			
T1–3	13	20.68 ± 36.41	0.196
T4	37	17.67 ± 26.78	
N stage			
N0	28	18.03 ± 32.42	0.358
N+	22	19.0 ± 25.29	

Table 1. *Cont.*

Parameter	N	Mean of PMB ± SD	*p*-Value
Clinical stage			
I–III	11	9.89 ± 27.75	0.019
IV	39	20.87 ± 29.47	
Metastasis			
No	41	14.23 ± 33.22	0.002
Yes	9	37.7 ± 19.32	
Perineural invasion			
No	33	20.79 ± 28.25	0.616
Yes	17	13.92 ± 33.68	
Lymphovascular invasion			
No	39	17.56 ± 4.52	0.991
Yes	11	21.63 ± 10.15	
HPV status			
p16 negative	46	19.82 ± 30.08	0.391
p16 positive	4	2.67 ± 1.00	

Two groups were compared using Mann–Whitney U tests. The Bonferroni-adjusted threshold for significance is set at $\alpha = 0.006$ (0.05/9).

2.2. cfDNA WES

WES data (cfDNA and matched normal samples) were obtained for all patients with a mean coverage depth of 90.87× and high coverage uniformity (98.18% of amplicons covered at 10× mean coverage). The WES data analysis flowchart is shown in Figure 1. The tools Muse, Mutect2, SomaticSniper, Sterlka2, and VarDict were used for variant calling to identify somatic mutations in the 50 paired cfDNA/normal samples and found 28,876, 1993, 21,763, 45,100, and 44,506 somatic mutations, respectively, with 84,365 somatic mutations found in total in the target (coding and splicing) region (Figure 1).

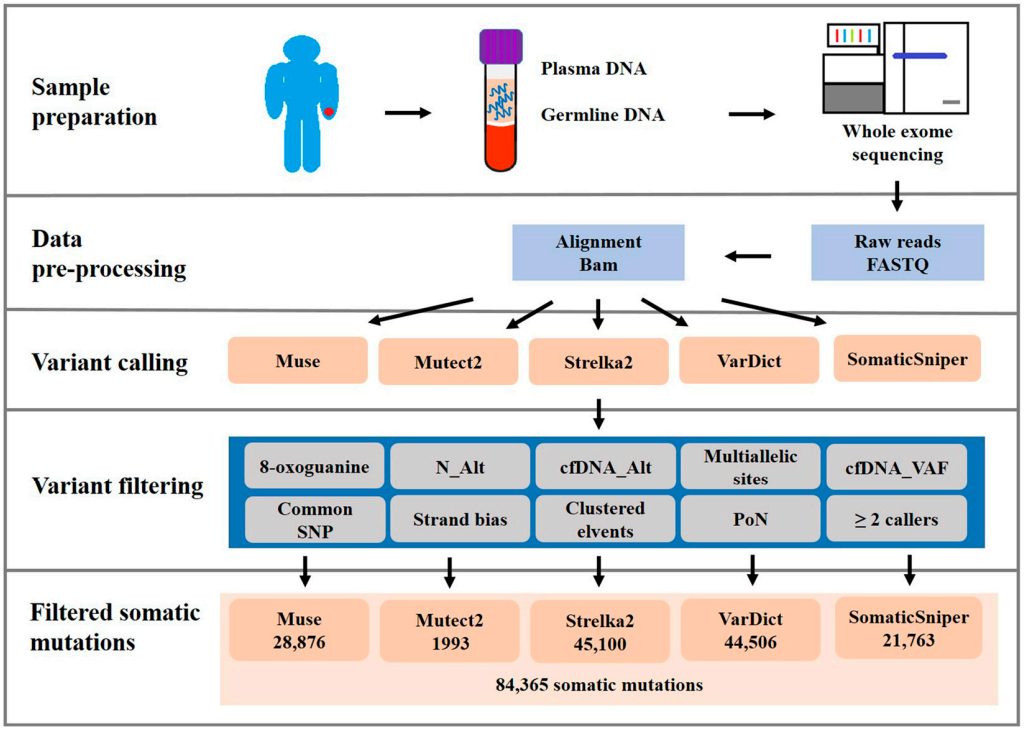

Figure 1. Flowchart illustrating the whole-exome sequencing (WES) analysis of cfDNA. WES of cfDNA was performed with matched normal samples from 50 OSCC patients. Somatic mutations were identified using five callers. The number of mutations called by each variant caller is depicted.

2.3. Validation and Assessment of Somatic Mutation Calling

IGV was used to examine somatic mutations in the frequently mutated genes according to the previous study [18,31,32]. The IGV screenshot shows somatic mutations that passed or did not pass the IGV examination (Supplementary Figure S3). IGV-passed mutations were represented in the Supplementary Figure S3A,C,E. Base calls with ≥2 mismatches with in a 20 bp window were considered false-positive mutations (Supplementary Figure S3B,D,F). As shown in Table 2, the most frequently observed non-PASS genes during IGV examination were *MUC19* (49.1%), *OBSCN* (38.5%), *KMT2D* (35.5%), *RYR1* (23.5%), and *MUC16* (22.5%). The high mutation levels of genes were correlated with high false-positive variants (Spearman's rho = 0.763, $p < 0.001$). Moreover, the loci of *MUC16* and *MUC19* had numerous recurrent false-positive variants in both cfDNA and normal samples (Supplementary Figure S4). Therefore, we filtered out the *MUC16* and *MUC19* mutations to reduce false-positive calls. After filtering, 84,045 somatic mutations remained in 14,733 unique genes, including 22,394 synonymous mutations, 54,310 missense mutations, 1136 splicing site mutations, 7 frameshift mutations, 22 in-frame mutations, 97 lost starts, 5982 inserted stops, 90 stop loss mutations, and 7 retained stops.

Table 2. Detection of false-positive mutations in the most frequently mutated genes.

Gene	Total Mutations	IGV PASS Mutations (%)		IGV Non-PASS Mutations (%)	
MUC19	57	29	(50.9%)	28	(49.1%)
OBSCN	78	48	(61.5%)	30	(38.5%)
KMT2D	62	40	(64.5%)	22	(35.5%)
RYR1	51	39	(76.5%)	12	(23.5%)
MUC16	111	86	(77.5%)	25	(22.5%)
DNAH1	50	39	(78.0%)	11	(22.0%)
PLEC	51	40	(78.4%)	11	(21.6%)
DNHD1	39	31	(79.5%)	8	(20.5%)
MACF1	56	45	(80.4%)	11	(19.6%)
USH2A	37	30	(81.1%)	7	(18.9%)
UBR4	57	47	(82.5%)	10	(17.5%)
FAT4	35	29	(82.9%)	6	(17.1%)
SYNE2	53	44	(83.0%)	9	(17.0%)
LRP1	43	36	(83.7%)	7	(16.3%)
LRP1B	44	37	(84.1%)	7	(15.9%)
HECTD4	47	40	(85.1%)	7	(14.9%)
INTS1	30	26	(86.7%)	4	(13.3%)
SYNE1	87	78	(89.7%)	9	(10.3%)
RYR3	62	56	(90.3%)	6	(9.7%)
TTN	116	105	(90.5%)	11	(9.5%)
DMD	48	44	(91.7%)	4	(8.3%)
ATM	36	33	(91.7%)	3	(8.3%)
DNAH11	39	36	(92.3%)	3	(7.7%)
NBEAL1	26	24	(92.3%)	2	(7.7%)
MYCBP2	40	37	(92.5%)	3	(7.5%)

2.4. Correlations between Mutation Burden and Sequencing Quality and Clinical Parameters

Plasma cfDNA mutation burden (PMB) was calculated as the number of somatic mutations at a VAF of ≥5% in the coding region per Mb. The mean PMB was 18.46 mutations per Mb per patient. As depicted in Supplementary Figure S2, PMB was a low/moderate correlation between cfDNA concentration (Spearman's rho = 0.328, $p = 0.020$) and 0.2× mean coverage (Spearman's rho = (–)0.320, $p = 0.023$). Although PMB was negatively correlated with coverage uniformity, all WES data showed better coverage uniformity (mean of 0.2× mean coverage: 98.18 ± 0.97%; range: 93–99%; Supplementary Figure S2D). A high PMB was strongly associated with distant metastasis ($p = 0.002$) and an advanced clinical stage ($p = 0.019$) (Table 1 and Figure 2). However, only the difference in distant metastasis was significant after Bonferroni correction. After adjusting for the effect of age, distant metastasis was also associated with PMB in Table S1 (B = 0.320, $p = 0.025$).

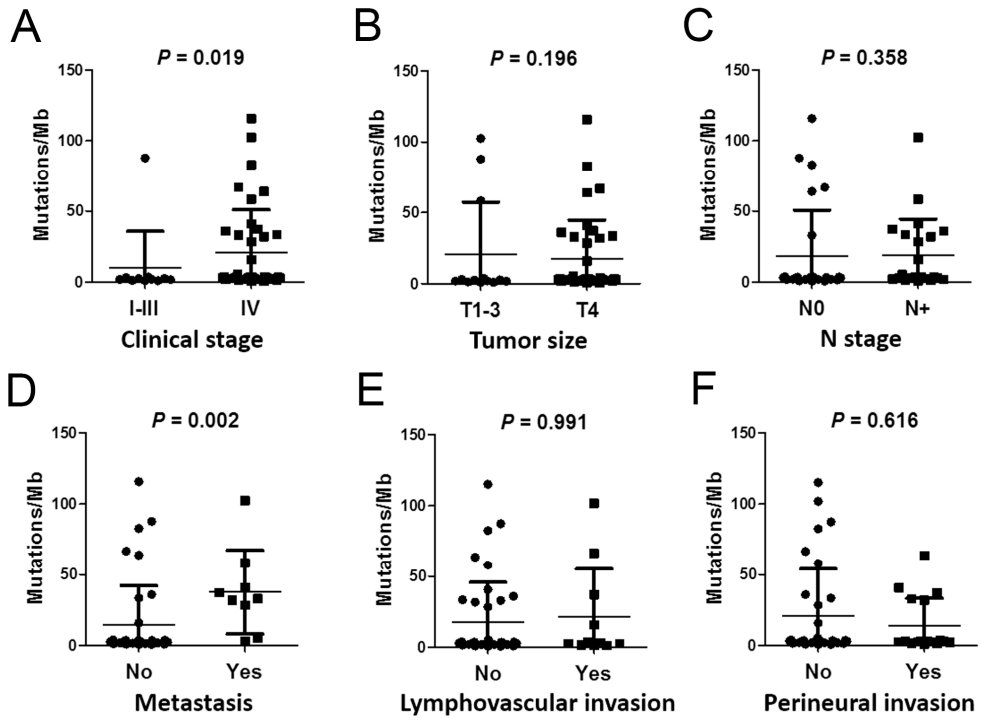

Figure 2. Scatter dot plot to illustrate the differential PMB associated with clinical parameters. Analysis of the PMB in OSCC patients according to (**A**) clinical stage, (**B**) tumor size, (**C**) N stage, (**D**) metastasis, (**E**) lymphovascular invasion, and (**F**) perineural invasion status. Each dot/square represent one sample value.

We further investigated the relationship between different mutation types and clinical parameters. As shown in Table 3, higher number of missense and splicing site mutations were significantly associated with advanced clinical stage ($p = 0.013$ and $p = 0.006$, respectively). However, none of these differences remained significant after Bonferroni correction. Higher number of synonymous, missense, inserted stop, splicing site, stop loss and loss start mutation were significantly associated with advanced clinical stage ($p = 0.003$, $p = 0.002$, $p = 0.003$, $p = 0.001$, $p = 0.023$ and $p = 0.001$, respectively). However, only the difference in synonymous, missense, inserted stop, splicing site, and loss start mutation were significant after Bonferroni correction.

Table 3. Association between mutation types and clinical parameters.

	Clinical Stage			Metastasis		
Mutation Types	**I–III**	**IV**	***p* Value**	**No**	**Yes**	***p* Value**
Synonymous mutations	234.7 ± 174.7	508.0 ± 115.4	0.089	350.1 ± 105.0	893.3 ± 219.6	0.003
Missense mutations	572.9 ± 449.7	1231.0 ± 279.6	0.013	832.4 ± 249.0	2242.4 ± 594.1	0.002
Inserted stop mutations	80.5 ± 71.6	130.7 ± 37.9	0.083	92.3 ± 36.2	244.2 ± 74.4	0.003
Splicing site mutations	10.0 ± 8.6	26.3 ± 6.0	0.006	17.5 ± 5.5	46.3 ± 10.6	0.001
Stop loss mutations	1.0 ± 0.8	2.0 ± 0.8	0.264	1.7 ± 0.7	2.3 ± 0.9	0.023
Lost start mutations	1.5 ± 1.5	2.1 ± 0.6	0.055	1.6 ± 0.6	3.6 ± 0.8	0.001
Retained stop mutations	0.0 ± 0.0	0.2 ± 0.1	0.170	0.1 ± 0.1	0.1 ± 0.1	0.911
In-frame mutations	0.2 ± 0.1	0.5 ± 0.1	0.327	0.4 ± 0.1	0.8 ± 0.4	0.200
Frameshift mutations	0.0 ± 0.0	0.2 ± 0.1	0.170	0.1 ± 0.1	0.2 ± 0.1	0.324

The Bonferroni-adjusted threshold for significance is set at $\alpha = 0.006$ (0.05/9).

2.5. Analysis of Plasma cfDNA Revealed Clinically Actionable Mutations without Prior Knowledge of the Tumor

Analysis of the cfDNA WES data indicated that the most frequently mutated genes were *TTN* (48%), *PLEC* (46%), *SYNE1* (44%), and *RYR3* (44%) (Figure 3). To predict the

potential mutational driver genes in OSCC, the InToGene platform and the datasets of Bailey et al. were used [33]. Four cancer driver genes, namely *KMT2D*, *LRP1B*, *TRRAP,* and *FLNA*, were identified in the 20 most frequently mutated gene sets. In the TCGA-OSCC dataset, the most frequently mutated genes having been observed were *TP53* (68%), *TTN* (42%), *FAT1* (26%), and *CDKN2A* (22%) (Table S2). The mutational landscape in our cfDNA appeared dissimilar to that in the TCGA-OSCC dataset (Table S3). In addition, we compared the TCGA-OSCC mutation profiles with our data. The novel mutated genes *CCDC168*, *HMCN2, STARD9*, and *CRAMP1* were significantly and frequently present in patients with OSCC. The mutation frequencies of *CCDC168*, *HMCN2, STARD9*, and *CRAMP1* were 34%, 32%, 32%, and 30%, respectively.

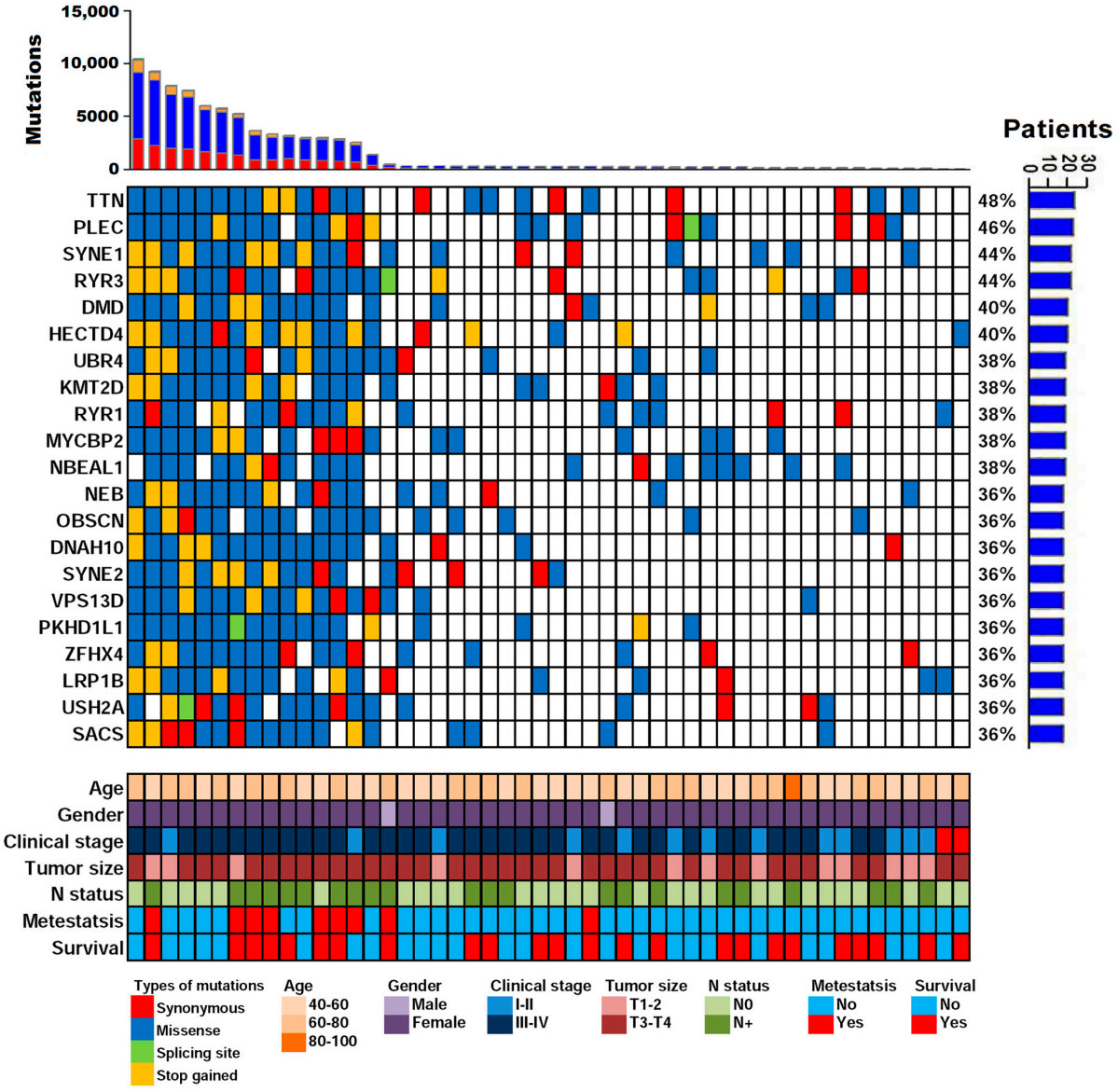

Figure 3. Mutation distribution of the most frequently mutated genes in cfDNA. Each column represents an individual OSCC patient, whereas each row denotes a mutated gene and clinical features. Clinical features and mutation types are color-coded as indicated. The panel on the right shows the number of mutations in the indicated gene.

The relationship between nonsynonymous mutations and clinical parameters was also examined in the 20 most frequently mutated genes. The presence of metastasis in patients with OSCC was significantly associated with nonsynonymous mutations in *TTN*, *SYNE1*,

RYR3, *DMD*, *HECTD4*, *KMT2D*, *NEB*, *DNAH10*, *SYNE2*, *VPS13D*, *ZFHX4*, and *LRP1B* (Table S4). However, only the difference in *KMT2D* and *DNAH10* were significant after Bonferroni correction. Kaplan–Meier survival curve analysis revealed that the mutation of *KMT2D* tended toward an association with a poor outcome, but the association was not significant (log rank $p = 0.090$). Moreover, no significant association was found between the gene mutations and other clinical parameters. Several of these genes are known to be involved in tumorigenesis, including *SYNE1, RYR3, HECTD4, KMT2D,* and *LRP1B* [34–38]. Furthermore, mutations in *TTN*, *KMT2D*, *ZFHX4*, and *LRP1B* are associated with poor outcomes [39–41].

The 300 most frequently mutated gene sets in the cfDNA WES data were used to conduct protein–protein interaction (PPI) network analysis and identify hub genes (Table S5). *KMT2A*, *CREBBP*, *MTOR,* and *ITPR1* were identified as hub genes with the highest predicted probability of controlling different gene clusters in cfDNA (Supplementary Figure S5A). These genes are involved in the regulation of chromatin-mediated transcription (*KMT2A*, *KMT2C*, and *KMT2D),* fundamental signal transduction (*MTOR*), and calcium signaling (*ITPR1*, *ITPR2*, and *ITPR3*). In addition, the dysregulation or mutation of these genes in cancer cells affects cell growth, survival, metabolism, and metastasis [41–44].

2.6. Distant Metastasis and Survival-Related Genes

We noted the significantly altered mutation frequency of genes between patients with distant metastatic OSCC and nonmetastatic OSCC (Figure 4A). *UMOD* was the most frequently mutated gene in patients with nonmetastatic OSCC, whereas *RORC*, *SLC49A3*, and *NUMBL* were the most frequently mutated genes in patients with metastatic OSCC. Deregulation expression of NUMBL and RORC have been reported to be involved in the regulation of cancer cell migration, invasion, and metastasis [45,46]. However, the role of *SLC49A3* in cancer is unclear. To identify the genetic mechanisms associated with metastasis, the 200 most frequently mutated gene sets in patients with metastatic OSCC were used to conduct PPI network analysis, which revealed that *NCOA1* and *CBL* were regulators with the highest predicted probability of controlling different gene clusters (Supplementary Figure S5B). *NCOA1* and *CBL* have previously been shown to play oncogenic roles in many cancers [47,48].

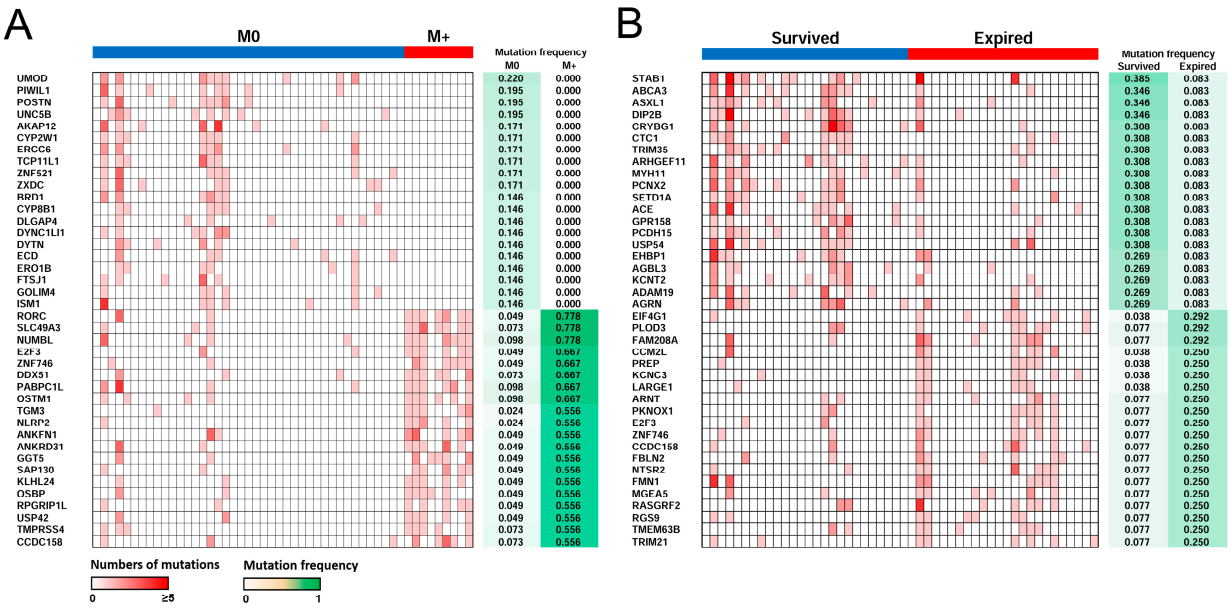

Figure 4. Heatmap of mutation profiles in cfDNA WES data according to metastasis and survival status. (**A**) The most frequently mutated genes in patients with metastatic and nonmetastatic OSCC are represented graphically. (**B**) Heatmap of the most frequently mutated genes in survived and expired patients. Panel on the right shows the frequency of mutations in the indicated gene.

The significantly altered mutation frequency of genes between surviving and expired patients is shown in Figure 4B. The most frequently mutated gene in patients that survived OSCC was *STAB1*, whereas the most frequently mutated genes in expired patients were *EIF4G1*, *PLOD3*, and *FAM208A*. *STAB1*, *EIF4G1*, and *PLOD3* have been reported to regulate the proliferation, migration, and invasion of cancer cells [49–51]; however, the role of *FAM208A* in cancer is unclear. A PPI network of proteins encoded by the 300 most frequently mutated gene sets in expired patients was constructed, and four hubs (*VCP, PPP2R1A, EHHADH,* and *ACAT1*) were identified (Supplementary Figure S5C). Mutations of *PPP2R1A* in uterine cancer affect oncogenic signaling and promote tumor cell growth [52], whereas *EHHADH* and *ACAT1* are regulators of drug resistance in tumor cells [53,54]; however, the role of *VCP* in cancer is unclear.

2.7. Molecular Pathway Analysis

The 300 most frequently mutated genes in all patients, patients with metastatic OSCC, and expired patients were imported into Annotation, Visualization and Integrated Discovery (DAVID) database, and Kyoto Encyclopedia of Genes and Genomes (KEGG) pathway enrichment analysis was performed. As shown in Table 4, the top three enriched KEGG pathways in all patients, namely extracellular matrix (ECM)-receptor interaction, the calcium signaling pathway, and the Notch signaling pathway, had a significant false discovery rate ($p < 0.05$). The top three enriched KEGG pathways in patients with metastatic OSCC were choline metabolism in cancer, O-glycan biosynthesis, and protein processing in the endoplasmic reticulum. The top three enriched KEGG pathways in expired patients were branched-chain amino acid (BCAA) catabolism, ECM-receptor interaction, and renal cell carcinoma. The genes in renal cell carcinoma are involved in the regulation of the hypoxia response; thus, these genes were considered a hypoxia-related gene set.

Table 4. Most frequently mutated molecules in all patients, patients with metastatic OSCC, and expired patients.

KEGG Pathway	FDR *p*-Value	Molecules
All Patients		
ECM-receptor interaction	<0.001	FRAS1, COL4A4, COL4A6, COL6A3, COL6A5, HSPG2, LAMA2, LAMA3, TNXB, VWF
Calcium signaling pathway	0.002	ATP2B3, CACNA1B, CACNA1D, CACNA1G, ERBB4, ITPR1, ITPR2, PHKB, RYR1, RYR2, RYR3
Notch signaling pathway	0.017	CREBBP, NOTCH1, NOTCH2, NOTCH4, NCOR2
Patients with metastatic OSCC		
Choline metabolism in cancer	0.018	RAF1, SP1, WAS, DGKK, DGKQ, DGKZ, PIK3CB, SLC22A3, SLC44A1, SLC44A2
O-glycan biosynthesis	0.019	RFNG, ST6GAL1, GALNT14, GALNT18, GALNT5, GALNT8
Protein processing in endoplasmic reticulum	0.044	DNAJC10, NPLOC4, SEC23B, SEL1L, SEL1L2, STT3A, TRAF2, UGGT2, EIF2AK1, HSPA4L, P4HB, PDIA4, VCP
Expired patients		
BCAA catabolism	0.022	HMGCS2, AUH, ACAT1, ACADSB, EHHADH
ECM-receptor interaction	0.036	AGRN, COL2A1, COL9A1, ITGA9, ITGB5, LAMC1
Hypoxia-related	0.042	ARNT, EPAS1, PAK3, RAF1, TFE3

The Kaplan–Meier method was used to analyze the association between OS time and the mutations of genes in these KEGG pathways. Mutations in *UGGT2*, *HSPA4L*, *COL2A1*, *AUH*, *ACADSB*, *ARNT*, *EPAS1*, *PAK3*, and *TFE3* were associated with poor outcomes (Supplementary Figure S6). However, only the difference in *HSPA4L* and *ACADSB* were significant after Bonferroni correction. Mutations in the BCAA catabolism gene set were detected in 12 (24%) patients (Figure 5A). Mutations in the calcium signaling-related genes *HMGCS2*, *AUH*, *ACAT1*, *ACADSB*, and *EHHADH* were found in 6 (12%), 6 (12%), 6 (12%), 4 (8%), and 5 (10%) patients, respectively (Supplementary Figure S7A). When patients had mutations in the BCAA catabolism gene set, their prognosis was poorer than that of

patients without such mutations. However, the difference in the BCAA catabolism gene set was not significant after Bonferroni correction. Mutations in the hypoxia-related gene set were found in 15 (30%) patients (Figure 5B); the affected genes were *ARNT*, *EPAS1*, *PAK3*, *RAF1*, and *TFE3* in 8 (16%), 4 (8%), 5 (10%), 6 (12%), and 7 (14%) patients, respectively (Supplementary Figure S7B). When patients had mutations in the hypoxia-related gene set, their prognosis was poorer than that of patients without such mutations. The difference in the hypoxia-related gene set remained significant after Bonferroni correction. We also identified Food and Drug Administration (FDA) approved drugs associated with the candidate genes. Two candidate genes, *HADHA* and *HADHB*, which are involved in the regulation of the BCAA catabolism pathway (Supplementary Figure S7A), were found to be susceptible to treatment with the FDA-approved drug triheptanoin.

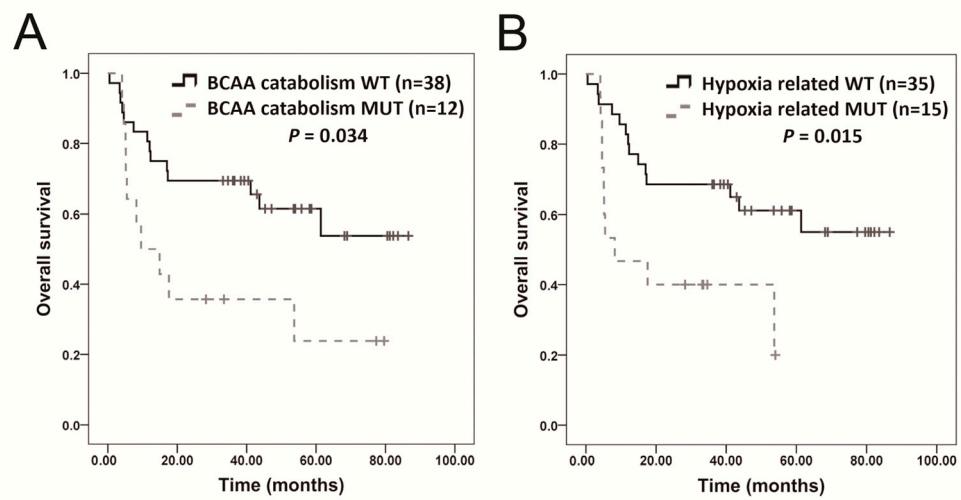

Figure 5. Mutations in branched-chain amino acid (BCAA) catabolism and hypoxia-related pathways are associated with patient survival. (**A**) Kaplan–Meier overall survival for patients with BCAA catabolism-mutated OSCC versus wild-type (WT) patients. (**B**) Kaplan–Meier overall survival for patients with hypoxia-related pathway-mutated OSCC versus WT OSCC. The Bonferroni-adjusted threshold for significance is set at $\alpha = 0.025$ (0.05/2).

3. Discussion

When using commonly available WES technologies, large amounts of circulating DNA are needed, which cannot be obtained from adequate volumes of plasma samples. In WES based on hybridization, the amount of circulating DNA and the complexity of the sequencing library can limit the process since a higher number of PCR cycles is required when the input material is limited. To address this issue, we utilized the ThruPLEX-FD Prep Kit (Rubicon Genomics, Inc., Ann Arbor, MI, USA) to maximize the yield for library generation [55–57]. cfDNA is usually present at low concentrations and highly fragmented, and its abundance depends on the cancer type and stage, as well as the sample treatment prior to analysis [58,59]. Shearing and other fragmentation methods have a considerable effect on the size distribution within fragments and therefore the results of analysis. Given the complexity of the complete workflow, including the preparation of samples and libraries, sequencing, and data analysis, the process should be standardized to ensure that data quality is optimized, especially when clinical cohorts are investigated [60]. The ThruPLEX system has high sensitivity, making possible the detection of more low-abundance somatic mutations than can be detected with QIAseq (Qiagen, Hilden, Germany), NEXTFLEX (BioScientific, Austin, TX, USA), Accel (Swift Biosciences, Ann Arbor, MI, USA) with PCR, and Accel PCR-freer kits [60]. Moreover, the ThruPLEX kit also allows the analysis of variants from various types of plasma samples [60]. In the present study, we combined library preparation via ThruPLEX-FD with exome enrichment via SureSelect technology to achieve 98.18% coverage and 90.87-fold depth. Our evaluation of cfDNA sequencing data

demonstrates the high performance of the established workflow combining ThruPLEX-FD library preparation with SureSelect technology for exome enrichment. To broaden the detection range of mutations, we employed the NGS technology platform (Illumina, San Diego, CA, USA) with high depth of sequences of the whole exon region. We obtained better mapping performance, enrichment efficiency, target coverage, and sequencing depth between cfDNA reads than another study with a depth of 49× (minimum: 40×) and exome coverage of 82% [21]. Another study was performed with a median sequencing depth of 55.59-fold for cfDNA WES [61]. Nonetheless, potential sources of error, such as content bias depending on the library generation method and amplification errors, must be considered. Addressing these potential sources of error through assay design should be considered during the design phase of experiments [62].

Whole-genome sequencing and WES of cfDNA have the potential to detect genetic variation at the nucleotide level, which could enable identification of subclonal tumors [63]. However, not all mutations found in plasma cfDNA necessarily originate from tumors. For instance, Dietz et al. reported a limited correlation (∼5–57%; median: 17.2%) between somatic cfDNA mutations and matched tumor samples in non-small cell lung cancer patients [57]. In contrast, other studies have found 11–92% of tissue mutations in the plasma of patients with HNSCC [30,64,65]. The source of this variation could include non-sampled tumor populations, distant metastases, or normal cells unrelated to the tumor. While germline variability can be filtered out by comparing with individually matched germline DNA and using databases like dbSNP (as done in this study), the specificity of cfDNA genomics will remain a challenge until more is known about the genetic aberrations in normal tissue and their representation in cfDNA [10]. The observation that the opposite was observed in HNSCC patients requires validation in a larger patient cohort.

In this study, we demonstrated the utility of WES for identifying cfDNA variants in plasma samples from cancer patients. Somatic mutations, including SNPs and known annotated mutations from the COSMIC database, were identified and removed from the datasets [18,66]. Germline variability was eliminated by comparing the data with individually matched germline DNA and applying high-fidelity filtering against databases such as dbSNP, PoN panel, oxodG artifacts, and strand bias [18,66]. To identify true somatic mutations, it is useful to combine the results of multiple mutation callers to reduce false positives while maintaining analysis sensitivity [67]. However, false-positive mutations may still be present in the datasets, even when normal panel SNPs and repeat-rich sequences have been removed [66]. IGV validation revealed false positives in some genes, particularly in gene variants with high mutation levels. A combination of at least two callers provides better performance than a single caller alone, based on the number of true and false detections in any combination of mutation callers across all replicates [18,66,67].

In the present study, we explored the relevance of using liquid biopsy to characterize the mutational landscape of OSCC using WES with deep coverage. We detected numerous different novel mutations at low frequencies in pathways possibly associated with OSCC oncogenesis. These included ECM-receptor interaction [68], arginine and proline metabolism [69], deregulated choline metabolism [70], and branched-chain amino acid metabolism [71]. Concordance between the variants determined by sequencing tumor tissue and cfDNA was low in previous studies [30,65]. Recurrent hotspot mutations in specific genes identified using a highly sensitive amplification-based method weas shown to have a higher sensitivity in OSCC [28]. Although the complete molecular landscape and tumor heterogeneity of OSCC are not yet fully understood, WES gene panels, such as the one used in this study, can provide a more comprehensive dataset of mutated genes in samples, as opposed to targeted panels that include only a limited number of genes [29,72–76]. This approach has the potential to identify genes of interest related to treatment resistance and capture DNA signatures that can help make treatment-related decisions without prior knowledge of the mutational profile [19,61].

Our data were discriminative from the TCGA database. In metastatic colon rectum cancer, gastric cancer, and endometrial carcinoma, cfDNA gene mutation patterns were

quite different when compared with the TCGA dataset [77–79]. This may results from the difference of sample patterns for patients enrolled in the studies. Asian patient cases are underrepresented in the TCGA, which are almost entirely non-metastatic surgical tissue samples. This may cause the discrepancy from the cfDNA scheme compared with the TCGA molecular classification scheme.

The level of cfDNA in the blood circulation can be affected by various factors, including tumor size, stage, and growth rate. The broader and deeper the cfDNA assay employed, the higher the likelihood of detecting mutations [20]. In addition, the total number of tumor-derived mutations interrogated is another important factor affecting the detection of mutation burdens in plasma. Higher levels of cfDNA in the blood circulation have been observed primarily in patients with a tumoral mass rather than patients without tumors [15]. In the case of OSCC, plasma cfDNA levels were significantly higher in patients with larger tumors, cervical lymph node metastasis, and late-stage cancer. These levels were also positively correlated with poor prognosis [15]. Thus, the level of cfDNA reflects tumor progression to some extent. In the present study, PMB was correlated with plasma concentration. The levels of cfDNA were significantly higher in patients with a higher PMB, a phenomenon that was also observed in hepatocellular carcinoma [61]. The mutational burden of cfDNA has been related to tumor size, tumor growth rate, or cell turnover, as shown using a theoretical mathematical model of cfDNA shedding in lung cancer [80]. In our study, higher PMB was significantly associated with unfavorable clinical parameter such as distant metastasis, after Bonferroni correction. However, our statistical power was less than 0.8 (power = 0.61); therefore, we could not eliminate the possibility of a type 2 error. The power analysis revealed that the sample size of N = 78 was required to achieve 80% power.

In particular, high levels of PMB were found in patients with distant metastatic OSCC. Similar findings were reported for rectal cancer, in which presurgery cfDNA was used to detect patients with minimal metastatic disease and identify those at high risk of distant recurrence [81]. This issue should be investigated further by collecting and analyzing more samples.

Previous studies have shown that tumor-derived cfDNA can be detected in 73% of patients with metastatic breast and prostate cancer, but cfDNA sensitivity in the metastatic setting may vary based on the location of the disease [81–83]. The ability of HNSCC tumor cells to metastasize depends on their ability to detach from the basement membrane and associated ECM components [84]. However, obtaining tumor biopsies can be limited by the location and timing of the biopsy, differential release of cfDNA among lesions, and tumor heterogeneity, which may limit the detection of tumor mutations [85,86]. The current study demonstrates that WES can be performed in a significant proportion of patients with metastatic oral cancers, enabling comprehensive clonal analysis of cfDNA to track tumor evolution and identify mechanisms of metastasis. It may be possible to develop a predictive algorithm that accurately distinguishes between metastatic and nonmetastatic cancer and identifies molecular-level mutational tumor types. Oncologists must rapidly screen for an increasing number of disease-specific or tumor agnostic biomarkers of drug response, but inadequate tumor tissue for comprehensive tumor profiling may delay appropriate systemic therapy administration. Patients with metastatic OSCC, which is difficult to biopsy, may be at risk of not receiving the most effective targeted therapies or curative immunotherapies. Liquid biopsies may soon be used to detect recurrent disease and select patients with OSCC for screening of distant metastasis during follow-up.

The mutational profile of a tumor plays a crucial role in determining the success of various therapeutic approaches, and precise targeting of these alterations, in combination with modified treatment regimens to reduce therapy resistance, can save many patients from disease and associated death. WES can identify mutations not included in targeted panels or global genomic features for samples with a high cfDNA tumor fraction. A more focused, sensitive assay capable of detecting clinically actionable mutations in cfDNA samples with low tumor fraction could also be employed. We believe this strategy will be

of widespread interest as cfDNA profiling may become the initial tumor sequencing assay for many OSCC patients, enabling rapid identification of actionable drug targets before therapy initiation [87]. However, the clinical feasibility of such approaches is limited by the low fraction of cfDNA derived from tumors and the high cost of WES. Moreover, while more sensitive but focused cfDNA platforms can detect clinically actionable mutations covered by the assay design, they may not be able to detect low-frequency mutations in genes where the functional consequences of mutation remain unclear. Therefore, testing new compounds to target these genes may be necessary to improve the prognosis of OSCC.

4. Materials and Methods

4.1. Participants and Data Collection

Fifty patients with OSCC were enrolled in our study, which was approved by the institutional review board of MacKay Memorial Hospital (approval numbers: 12MMHIS178 and 15MMHIS104), after the patients provided informed consent. Demographic data, i.e., age, sex, clinical stage, and final status (survived or expired), were obtained from the patients' medical records. For clinical staging, the tumor, node, and metastasis TNM classification of the American Joint Committee on Cancer (AJCC 7th edition) were used [88]. Exclusion criteria for this study were receiving adjuvant chemotherapy or radiotherapy before surgery.

TCGA-HNSCC WES dataset was downloaded from the Genomic Data Commons portal (https://portal.gdc.cancer.gov/) (accessed on 25 December 2021). We included only 387 patients where the primary site was located at the tongue, lip, mouth floor, tonsil, gums, palate, or oropharynx. This dataset was called "TCGA-OSCC" dataset [18]. Mutations located in the introns, intergenic regions, and in untranslated regions (UTR) were excluded.

4.2. DNA Extraction

cfDNA was extracted from 2 mL of plasma (obtained before OSCC-associated surgery) using a QIAamp Circulating Nucleic Acid Kit (Qiagen), as described previously [15]. Purified cfDNA was then eluted in 25 µL of elution buffer from the kit. The QIAamp Nucleic Acid Kit was used for sample collection instead of simple EDTA-coated tubes and blood samples were centrifuged immediately to avoid DNA fragmentation, which may achieve the best preservation of circulating cfDNA. cfDNA was quantified using a TapeStation 2200 (Agilent Technologies, Santa Clara, CA, USA), equipped with a high sensitivity D1000 ScreenTape system. This system analyzes up to 96 samples per run and resolves 35–1000 bp fragments, and the assay is suitable for the accurate sizing and quantification of DNA fragments in high-throughput applications (Supplementary Figure S1A) [15]. Paired whole-blood samples were collected in EDTA Vacutainer tubes (Becton Dickinson, Franklin Lakes, NJ, USA). Peripheral blood mononuclear cell negative fractions were used for germline DNA. Germline DNA was extracted from buffy coat layer prepared from 10 mL of whole blood using a QIAamp DNA Blood Mini Kit (Qiagen) according to the manufacturer's instructions. The quality and quantity of genomic DNA were assessed using the TapeStation 2200 and a NanoDrop 2000 Photometer (Thermo Fisher Scientific, Waltham, MA, USA).

4.3. Sequencing of Plasma cfDNA

For plasma samples, ~1 ng of cfDNA was used as the input for library preparation, and libraries were prepared using a ThruPLEX DNA-seq Library Prep Kit according to the manufacturer's protocol. For blood samples, libraries were prepared with 200 ng of genomic DNA using a SureSelect Library Preparation Kit (Agilent Technologies) according to the manufacturer's instructions [21,55]. For exome enrichment, SureSelect Human All Exon V6 + UTRs probe sets were used. The captured libraries were amplified with 14 cycles of PCR, and the quality and concentration of libraries were assessed using the TapeStation 2200 system (Supplementary Figure S1B). Libraries were indexed with barcodes to allow

sample pooling for multiplexed exome capture and sequencing. An IlluminaNovaSeq 6000 DNA sequencer (Illumina) was used to conduct WES [18].

4.4. Sequencing Data Processing

Somatic mutations were called using multiple pipelines (Figure 1). Sequencing data were aligned to the human hg38 genome using Burrows-Wheeler Aligner (v0.7.15). The Sequence Alignment/Map (SAM) file format was converted to the Binary Alignment/Map (i.e., BAM) format with SAMtools (v1.3.1). Five programs were used to call somatic mutations: Muse (v1.0rc), Mutect2 (v4.1.0.0), Strelka2 (v2.9.10), SomaticSniper (v1.0.5.0), and VarDict (v1.8.3) [89–92]. Plasma cfDNA somatic mutations were called via comparisons with matched control germline DNA. After variant identification, the variant calling file data from the five programs were merged using sample IDs and positions in the genome (e.g., ID-chr1-123).

Data were further filtered using the criteria reported in our previous study [18]: (i) removing common polymorphisms (SNPs), a minor allele frequency in the 1000 Genomes Project or Genome Aggregation Database (gnomAD) of >1%; (ii) Panel of Normal (the normal panel was created with the GATK tool "CreateSomaticPanelOfNormals"); (iii) 8-oxoguanine artifacts (identified and filtered using the GATK tools "FilterByOrientationBias" and "CollectSequencingArtifactMetrics", respectively); (iv) removal of multiallelic sites, clustered events, and strand bias (estimated and filtered using the GATK tools "GetPileupSummaries," "FilterMutectCalls," and "CalculateContamination", respectively); (v) <4 mutant alleles in the cfDNA sample and ≥4 mutant alleles in normal cells [93]; and (vi) variant allele frequency (VAF) of <0.05 in cfDNA tumor samples. Steensma DP suggested that next-generation sequencing has a mutation limit of detection at VAFs ~2% [64,94]. The thresholds of VAF was defined as >2% in our study. The filtered mutations were considered somatic mutations.

Variant Effect Predictor (v106; Ensembl: https://asia.ensembl.org/Homo_sapiens/Tools/VEP) (accessed on 13 May 2021). was used to annotate the somatic mutations [95]. By searching the InToGene platform (https://www.intogen.org/search, accessed on 13 May 2021) and the Bailey et al. datasets [33,96], potential mutational driver genes in OSCC were identified and annotated. Germline DNA and cfDNA WES data described in the present study were submitted to the Short Reads Archive database under BioProject accession numbers PRJNA749133 (https://www.ncbi.nlm.nih.gov/bioproject/?term=PRJNA749133, accessed on 13 May 2021) and PRJNA759378 (https://www.ncbi.nlm.nih.gov/bioproject/?term=PRJNA759378, accessed on 13 May 2021), respectively.

The plasma cfDNA mutation burden (PMB) was calculated according to the number of somatic mutations with a VAF of ≥5% in the target region of SureSelect Human All Exon v6 + UTR [91.08 megabases (Mb)] and is expressed as mutations per Mb [97,98]. The target region of the BED file is available at the SureDesign website (https://earray.chem.agilent.com/suredesign/, accessed on 13 May 2021).

4.5. Validation of Mutations

IGV (v2.13.1) was used to validate somatic mutations [18,99,100]. The 200 most frequently mutated genes were selected, and IGV was used to determine false-positive rates. To be considered "true-positive," mutations were required to fulfill the following criteria: (i) the allelic configurations of the mutation were multiallelic variants; (ii) both forward and reverse strands had at least one mutant allele; (iii) <2 mismatches occurred within a 20 bp window; and (iv) the number of Alt alleles was <3 in normal cells and ≥3 in tumors [95].

4.6. Pathway Analysis

The 300 candidate genes with the highest mutation rates in all, metastatic, or expired patients were imported into a PPI network produced using STRING (v11.5; https://string-db.org/, accessed on 13 May 2021).

DAVID (https://david.ncifcrf.gov/, accessed on 13 May 2021) was used to further analyze the annotation results of the candidate genes. KEGG pathway functional enrichment results were analyzed using DAVID with a false discovery rate of <0.05.The candidate genes were matched with FDA–approved drugs (https://www.fda.gov/, accessed on 13 May 2021) using the United States FDA Table of Pharmacogenomic Biomarkers in Drug Labels.

4.7. Statistical Analysis

Data are presented as the SD ± standard deviation. For statistical analysis, rank correlation was conducted using Spearman and Mann–Whitney U tests. The categorical data was conducted by chi-square or Fisher's test (expected number less than 5). Linear regression models were used to assess the association between clinical stage and distant metastasis with PBM, adjusted for age. Overall survival (OS) was defined as the duration from the time of first diagnosis to death or the last date of follow-up. OS was compared between two groups using Kaplan–Meier analysis. p values of <0.05 were considered statistically significant. To adjust for multiple tests, the p value for significance was adjusted by Bonferroni correction.

5. Conclusions

Based on the findings of this study, an array of five mutation callers was utilized to identify mutations in cfDNA samples from OSCC patients. The presence of PMB mutations was found to be associated with advanced disease stage and distant metastasis. In addition, novel somatic mutations were detected in cfDNA samples from patients with metastatic OSCC. This information could potentially inform the use of precision therapy approaches tailored to the specific mutations identified in individual patients' cfDNA samples.

Supplementary Materials: The supporting information can be downloaded at: https://www.mdpi.com/article/10.3390/ijms241210408/s1.

Author Contributions: C.-J.L. contributed to supervision, conception and design, data acquisition, analysis, and interpretation, drafted and critically revised the manuscript; K.-W.C. contributed to supervision and drafted the manuscript; L.-H.L. contributed to data acquisition, analysis, and interpretation, drafted the manuscript; H.-W.C. contributed to lab work, data analysis, and interpretation. All authors have read and agreed to the published version of the manuscript.

Funding: This study was supported by grants from MacKay Memorial Hospital (MMH-E-105-12 and MMH-E-108-12) and the National Science and Technology Council (NSTC), Taiwan: (NSTC 108-2314-B-195-002-MY2, NSTC 105-2314-B-195-005-MY3 and 110-2314-B-195-015-MY3).

Institutional Review Board Statement: This study was approved by the institutional review board of MacKay Memorial Hospital (approval numbers: 12MMHIS178 and 15MMHIS104), after the patients provided informed consent.

Informed Consent Statement: Informed consent was obtained from all subjects involved in the study.

Data Availability Statement: All WES data described in the present study were submitted to the Short Reads Archive database (BioProject accession numbers: PRJNA749133 and PRJNA759378) and the SRA Run Selector project (https://www.ncbi.nlm.nih.gov/bioproject/?term=PRJNA749133 and https://www.ncbi.nlm.nih.gov/bioproject/?term=PRJNA759378).

Conflicts of Interest: The authors declare no potential conflicts of interest.

References

1. World Health Organization. *Cancer Today*, GLOBOCAN 2020th ed.; GLOBOCAN: Lyon, France, 2020; Volume 2020, pp. 1–2.
2. Boute, P.; Page, C.; Biet, A.; Cuvelier, P.; Strunski, V.; Chevalier, D. Epidemiology, prognosis and treatment of simultaneous squamous cell carcinomas of the oral cavity and hypopharynx. *Eur. Ann. Otorhinolaryngol. Head Neck Dis.* **2014**, *131*, 283–287. [CrossRef]
3. Gluckman, J.L. Synchronous multiple primary lesions of the upper aerodigestive system. *Arch. Otolaryngol.* **1979**, *105*, 597–598. [CrossRef]

4. Gupta, S.; Kong, W.; Peng, Y.; Miao, Q.; Mackillop, W.J. Temporal trends in the incidence and survival of cancers of the upper aerodigestive tract in Ontario and the United States. *Int. J. Cancer* **2009**, *125*, 2159–2165. [CrossRef]
5. Braakhuis, B.J.; Tabor, M.P.; Leemans, C.R.; van der Waal, I.; Snow, G.B.; Brakenhoff, R.H. Second primary tumors and field cancerization in oral and oropharyngeal cancer: Molecular techniques provide new insights and definitions. *Head Neck* **2002**, *24*, 198–206. [CrossRef]
6. Kidess, E.; Jeffrey, S.S. Circulating tumor cells versus tumor-derived cell-free DNA: Rivals or partners in cancer care in the era of single-cell analysis? *Genome Med.* **2013**, *5*, 70. [CrossRef] [PubMed]
7. Spellman, P.T.; Gray, J.W. Detecting cancer by monitoring circulating tumor DNA. *Nat. Med.* **2014**, *20*, 474–475. [CrossRef] [PubMed]
8. Bettegowda, C.; Sausen, M.; Leary, R.J.; Kinde, I.; Wang, Y.; Agrawal, N.; Bartlett, B.R.; Wang, H.; Luber, B.; Alani, R.M.; et al. Detection of circulating tumor DNA in early- and late-stage human malignancies. *Sci. Transl. Med.* **2014**, *6*, 224ra24. [CrossRef] [PubMed]
9. Wan, J.C.M.; Massie, C.; Garcia-Corbacho, J.; Mouliere, F.; Brenton, J.D.; Caldas, C.; Pacey, S.; Baird, R.; Rosenfeld, N. Liquid biopsies come of age: Towards implementation of circulating tumour DNA. *Nat. Rev. Cancer* **2017**, *17*, 223–238. [CrossRef] [PubMed]
10. Bardelli, A.; Pantel, K. Liquid Biopsies, What We Do Not Know (Yet). *Cancer Cell* **2017**, *31*, 172–179. [CrossRef] [PubMed]
11. Venesio, T.; Siravegna, G.; Bardelli, A.; Sapino, A. Liquid Biopsies for Monitoring Temporal Genomic Heterogeneity in Breast and Colon Cancers. *Pathobiology* **2018**, *85*, 146–154. [CrossRef]
12. Couraud, S.; Vaca-Paniagua, F.; Villar, S.; Oliver, J.; Schuster, T.; Blanche, H.; Girard, N.; Tredaniel, J.; Guilleminault, L.; Gervais, R.; et al. Noninvasive diagnosis of actionable mutations by deep sequencing of circulating free DNA in lung cancer from never-smokers: A proof-of-concept study from BioCAST/IFCT-1002. *Clin. Cancer Res.* **2014**, *20*, 4613–4624. [CrossRef] [PubMed]
13. Jung, K.; Fleischhacker, M.; Rabien, A. Cell-free DNA in the blood as a solid tumor biomarker—A critical appraisal of the literature. *Clin. Chim. Acta* **2010**, *411*, 1611–1624. [CrossRef] [PubMed]
14. Mazurek, A.M.; Rutkowski, T.; Fiszer-Kierzkowska, A.; Malusecka, E.; Skladowski, K. Assessment of the total cfDNA and HPV16/18 detection in plasma samples of head and neck squamous cell carcinoma patients. *Oral Oncol.* **2016**, *54*, 36–41. [CrossRef] [PubMed]
15. Lin, L.-H.; Chang, K.-W.; Kao, S.-Y.; Cheng, H.-W.; Liu, C.-J. Increased Plasma Circulating Cell-Free DNA Could Be a Potential Marker for Oral Cancer. *Int. J. Mol. Sci.* **2018**, *19*, 3303. [CrossRef]
16. Agrawal, N.; Frederick, M.J.; Pickering, C.R.; Bettegowda, C.; Chang, K.; Li, R.J.; Fakhry, C.; Xie, T.X.; Zhang, J.; Wang, J.; et al. Exome sequencing of head and neck squamous cell carcinoma reveals inactivating mutations in NOTCH1. *Science* **2011**, *333*, 1154–1157. [CrossRef]
17. Stransky, N.; Egloff, A.M.; Tward, A.D.; Kostic, A.D.; Cibulskis, K.; Sivachenko, A.; Kryukov, G.V.; Lawrence, M.S.; Sougnez, C.; McKenna, A.; et al. The mutational landscape of head and neck squamous cell carcinoma. *Science* **2011**, *333*, 1157–1160. [CrossRef]
18. Lin, L.-H.; Chou, C.-H.; Cheng, H.-W.; Chang, K.-W.; Liu, C.-J. Precise Identification of Recurrent Somatic Mutations in Oral Cancer through Whole-Exome Sequencing Using Multiple Mutation Calling Pipelines. *Front. Oncol.* **2021**, *11*, 741626. [CrossRef]
19. Bos, M.K.; Angus, L.; Nasserinejad, K.; Jager, A.; Jansen, M.; Martens, J.W.M.; Sleijfer, S. Whole exome sequencing of cell-free DNA—A systematic review and Bayesian individual patient data meta-analysis. *Cancer Treat. Rev.* **2020**, *83*, 101951. [CrossRef]
20. Tsui, D.W.Y.; Cheng, M.L.; Shady, M.; Yang, J.L.; Stephens, D.; Won, H.; Srinivasan, P.; Huberman, K.; Meng, F.; Jing, X.; et al. Tumor fraction-guided cell-free DNA profiling in metastatic solid tumor patients. *Genome Med.* **2021**, *13*, 96. [CrossRef]
21. Tailor, T.D.; Rao, X.; Campa, M.J.; Wang, J.; Gregory, S.G.; Patz, E.F., Jr. Whole Exome Sequencing of Cell-Free DNA for Early Lung Cancer: A Pilot Study to Differentiate Benign from Malignant CT-Detected Pulmonary Lesions. *Front. Oncol.* **2019**, *9*, 317. [CrossRef]
22. Cancer Genome Atlas, N. Comprehensive genomic characterization of head and neck squamous cell carcinomas. *Nature* **2015**, *517*, 576–582. [CrossRef] [PubMed]
23. Schmidt, H.; Kulasinghe, A.; Kenny, L.; Punyadeera, C. The development of a liquid biopsy for head and neck cancers. *Oral Oncol.* **2016**, *61*, 8–11. [CrossRef] [PubMed]
24. Schmidt, H.; Kulasinghe, A.; Allcock, R.J.N.; Tan, L.Y.; Mokany, E.; Kenny, L.; Punyadeera, C. A Pilot Study to Non-Invasively Track PIK3CA Mutation in Head and Neck Cancer. *Diagnostics* **2018**, *8*, 79. [CrossRef] [PubMed]
25. Nakagaki, T.; Tamura, M.; Kobashi, K.; Omori, A.; Koyama, R.; Idogawa, M.; Ogi, K.; Hiratsuka, H.; Tokino, T.; Sasaki, Y. Targeted next-generation sequencing of 50 cancer-related genes in Japanese patients with oral squamous cell carcinoma. *Tumour Biol.* **2018**, *40*, 1010428318800180. [CrossRef]
26. van Ginkel, J.H.; Huibers, M.M.H.; van Es, R.J.J.; de Bree, R.; Willems, S.M. Droplet digital PCR for detection and quantification of circulating tumor DNA in plasma of head and neck cancer patients. *BMC Cancer* **2017**, *17*, 428. [CrossRef] [PubMed]
27. Braig, F.; Voigtlaender, M.; Schieferdecker, A.; Busch, C.J.; Laban, S.; Grob, T.; Kriegs, M.; Knecht, R.; Bokemeyer, C.; Binder, M. Liquid biopsy monitoring uncovers acquired RAS-mediated resistance to cetuximab in a substantial proportion of patients with head and neck squamous cell carcinoma. *Oncotarget* **2016**, *7*, 42988–42995. [CrossRef]
28. Lin, L.-H.; Cheng, H.-W.; Liu, C.-J. Droplet digital polymerase chain reaction for detection and quantification of cell-free DNA TP53 target somatic mutations in oral cancer. *Cancer Biomark.* **2022**, *33*, 29–41. [CrossRef]
29. Yang, X.; Xu, X.; Zhang, C.; Ji, T.; Wan, T.; Liu, W. The diagnostic value and prospects of gene mutations in circulating tumor DNA for head and neck cancer monitoring. *Oral Oncol.* **2022**, *128*, 105846. [CrossRef]

30. Liebs, S.; Eder, T.; Klauschen, F.; Schutte, M.; Yaspo, M.-L.; Keilholz, U.; Tinhofer, I.; Kidess-Sigal, E.; Braunholz, D. Applicability of liquid biopsies to represent the mutational profile of tumor tissue from different cancer entities. *Oncogene* **2021**, *40*, 5204–5212. [CrossRef]
31. Glennon, K.I.; Maralani, M.; Abdian, N.; Paccard, A.; Montermini, L.; Nam, A.J.; Arseneault, M.; Staffa, A.; Jandaghi, P.; Meehan, B.; et al. Rational Development of Liquid Biopsy Analysis in Renal Cell Carcinoma. *Cancers* **2021**, *13*, 5825. [CrossRef]
32. Hata, T.; Mizuma, M.; Motoi, F.; Omori, Y.; Ishida, M.; Nakagawa, K.; Hayashi, H.; Morikawa, T.; Kamei, T.; Furukawa, T.; et al. GNAS mutation detection in circulating cell-free DNA is a specific predictor for intraductal papillary mucinous neoplasms of the pancreas, especially for intestinal subtype. *Sci. Rep.* **2020**, *10*, 17761. [CrossRef]
33. Bailey, M.H.; Tokheim, C.; Porta-Pardo, E.; Sengupta, S.; Bertrand, D.; Weerasinghe, A.; Colaprico, A.; Wendl, M.C.; Kim, J.; Reardon, B.; et al. Comprehensive Characterization of Cancer Driver Genes and Mutations. *Cell* **2018**, *173*, 371–385.e318. [CrossRef] [PubMed]
34. Faraj Shaglouf, L.H.; Ranjpour, M.; Wajid, S.; Jain, S.K. Elevated expression of cellular SYNE1, MMP10, and GTPase1 and their regulatory role in hepatocellular carcinoma progression. *Protoplasma* **2020**, *257*, 157–167. [CrossRef]
35. Abudureheman, A.; Ainiwaer, J.; Hou, Z.; Niyaz, M.; Turghun, A.; Hasim, A.; Zhang, H.; Lu, X.; Sheyhidin, I. High MLL2 expression predicts poor prognosis and promotes tumor progression by inducing EMT in esophageal squamous cell carcinoma. *J. Cancer Res. Clin. Oncol.* **2018**, *144*, 1025–1035. [CrossRef]
36. Ni, S.; Hu, J.; Duan, Y.; Shi, S.; Li, R.; Wu, H.; Qu, Y.; Li, Y. Down expression of LRP1B promotes cell migration via RhoA/Cdc42 pathway and actin cytoskeleton remodeling in renal cell cancer. *Cancer Sci.* **2013**, *104*, 817–825. [CrossRef] [PubMed]
37. Zhang, L.; Liu, Y.; Song, F.; Zheng, H.; Hu, L.; Lu, H.; Liu, P.; Hao, X.; Zhang, W.; Chen, K. Functional SNP in the microRNA-367 binding site in the 3'UTR of the calcium channel ryanodine receptor gene 3 (RYR3) affects breast cancer risk and calcification. *Proc. Natl. Acad. Sci. USA* **2011**, *108*, 13653–13658. [CrossRef]
38. Wan, T.; Wang, H.; Gou, M.; Si, H.; Wang, Z.; Yan, H.; Liu, T.; Chen, S.; Fan, R.; Qian, N.; et al. LncRNA HEIH promotes cell proliferation, migration and invasion in cholangiocarcinoma by modulating miR-98-5p/HECTD4. *Biomed. Pharmacother.* **2020**, *125*, 109916. [CrossRef] [PubMed]
39. Han, X.; Chen, J.; Wang, J.; Xu, J.; Liu, Y. TTN mutations predict a poor prognosis in patients with thyroid cancer. *Biosci. Rep.* **2022**, *42*, BSR20221168. [CrossRef] [PubMed]
40. Ardeshir-Larijani, F.; Bhateja, P.; Lipka, M.B.; Sharma, N.; Fu, P.; Dowlati, A. KMT2D Mutation Is Associated with Poor Prognosis in Non-Small-Cell Lung Cancer. *Clin. Lung Cancer* **2018**, *19*, e489–e501. [CrossRef]
41. Rao, R.C.; Dou, Y. Hijacked in cancer: The KMT2 (MLL) family of methyltransferases. *Nat. Rev. Cancer* **2015**, *15*, 334–346. [CrossRef]
42. Tang, Z.; Yu, W.; Zhang, C.; Zhao, S.; Yu, Z.; Xiao, X.; Tang, R.; Xuan, Y.; Yang, W.; Hao, J.; et al. CREB-binding protein regulates lung cancer growth by targeting MAPK and CPSF4 signaling pathway. *Mol. Oncol.* **2016**, *10*, 317–329. [CrossRef] [PubMed]
43. Tian, T.; Li, X.; Zhang, J. mTOR Signaling in Cancer and mTOR Inhibitors in Solid Tumor Targeting Therapy. *Int. J. Mol. Sci.* **2019**, *20*, 755. [CrossRef] [PubMed]
44. Kania, E.; Roest, G.; Vervliet, T.; Parys, J.B.; Bultynck, G. IP3 Receptor-Mediated Calcium Signaling and Its Role in Autophagy in Cancer. *Front. Oncol.* **2017**, *7*, 140. [CrossRef] [PubMed]
45. Vaira, V.; Faversani, A.; Martin, N.M.; Garlick, D.S.; Ferrero, S.; Nosotti, M.; Kissil, J.L.; Bosari, S.; Altieri, D.C. Regulation of lung cancer metastasis by Klf4-Numb-like signaling. *Cancer Res.* **2013**, *73*, 2695–2705. [CrossRef] [PubMed]
46. Cao, D.; Qi, Z.; Pang, Y.; Li, H.; Xie, H.; Wu, J.; Huang, Y.; Zhu, Y.; Shen, Y.; Zhu, Y.; et al. Retinoic Acid-Related Orphan Receptor C Regulates Proliferation, Glycolysis, and Chemoresistance via the PD-L1/ITGB6/STAT3 Signaling Axis in Bladder Cancer. *Cancer Res.* **2019**, *79*, 2604–2618. [CrossRef]
47. Wang, L.; Li, W.; Li, K.; Guo, Y.; Liu, D.; Yao, Z.; Lin, X.; Li, S.; Jiang, Z.; Liu, Q.; et al. The oncogenic roles of nuclear receptor coactivator 1 in human esophageal carcinoma. *Cancer Med.* **2018**, *7*, 5205–5216. [CrossRef]
48. Kang, J.M.; Park, S.; Kim, S.J.; Hong, H.Y.; Jeong, J.; Kim, H.S.; Kim, S.J. CBL enhances breast tumor formation by inhibiting tumor suppressive activity of TGF-beta signaling. *Oncogene* **2012**, *31*, 5123–5131. [CrossRef]
49. Baek, J.H.; Yun, H.S.; Kwon, G.T.; Kim, J.Y.; Lee, C.W.; Song, J.Y.; Um, H.D.; Kang, C.M.; Park, J.K.; Kim, J.S.; et al. PLOD3 promotes lung metastasis via regulation of STAT3. *Cell Death Dis.* **2018**, *9*, 1138. [CrossRef]
50. Lu, Y.; Yu, S.; Wang, G.; Ma, Z.; Fu, X.; Cao, Y.; Li, Q.; Xu, Z. Elevation of EIF4G1 promotes non-small cell lung cancer progression by activating mTOR signalling. *J. Cell. Mol. Med.* **2021**, *25*, 2994–3005. [CrossRef]
51. Glatzel-Plucinska, N.; Piotrowska, A.; Dziegiel, P.; Podhorska-Okolow, M. The Role of SATB1 in Tumour Progression and Metastasis. *Int. J. Mol. Sci.* **2019**, *20*, 4156. [CrossRef]
52. Haesen, D.; Abbasi Asbagh, L.; Derua, R.; Hubert, A.; Schrauwen, S.; Hoorne, Y.; Amant, F.; Waelkens, E.; Sablina, A.; Janssens, V. Recurrent PPP2R1A Mutations in Uterine Cancer Act through a Dominant-Negative Mechanism to Promote Malignant Cell Growth. *Cancer Res.* **2016**, *76*, 5719–5731. [CrossRef]
53. Okamura, S.; Yoshino, H.; Kuroshima, K.; Tsuruda, M.; Osako, Y.; Sakaguchi, T.; Yonemori, M.; Yamada, Y.; Tatarano, S.; Nakagawa, M.; et al. EHHADH contributes to cisplatin resistance through regulation by tumor-suppressive microRNAs in bladder cancer. *BMC Cancer* **2021**, *21*, 48. [CrossRef]
54. Ayyagari, V.N.; Wang, X.; Diaz-Sylvester, P.L.; Groesch, K.; Brard, L. Assessment of acyl-CoA cholesterol acyltransferase (ACAT-1) role in ovarian cancer progression-An in vitro study. *PLoS ONE* **2020**, *15*, e0228024. [CrossRef] [PubMed]

55. Murtaza, M.; Dawson, S.-J.; Tsui, D.W.; Gale, D.; Forshew, T.; Piskorz, A.M.; Parkinson, C.; Chin, S.-F.; Kingsbury, Z.; Wong, A.S.; et al. Non-invasive analysis of acquired resistance to cancer therapy by sequencing of plasma DNA. *Nature* **2013**, *497*, 108–112. [CrossRef] [PubMed]
56. Klevebring, D.; Neiman, M.; Sundling, S.; Eriksson, L.; Darai Ramqvist, E.; Celebioglu, F.; Czene, K.; Hall, P.; Egevad, L.; Gronberg, H.; et al. Evaluation of exome sequencing to estimate tumor burden in plasma. *PLoS ONE* **2014**, *9*, e104417. [CrossRef]
57. Dietz, S.; Schirmer, U.; Merce, C.; von Bubnoff, N.; Dahl, E.; Meister, M.; Muley, T.; Thomas, M.; Sultmann, H. Low Input Whole-Exome Sequencing to Determine the Representation of the Tumor Exome in Circulating DNA of Non-Small Cell Lung Cancer Patients. *PLoS ONE* **2016**, *11*, e0161012. [CrossRef] [PubMed]
58. Elazezy, M.; Joosse, S.A. Techniques of using circulating tumor DNA as a liquid biopsy component in cancer management. *Comput. Struct. Biotechnol. J.* **2018**, *16*, 370–378. [CrossRef]
59. Trigg, R.M.; Martinson, L.J.; Parpart-Li, S.; Shaw, J.A. Factors that influence quality and yield of circulating-free DNA: A systematic review of the methodology literature. *Heliyon* **2018**, *4*, e00699. [CrossRef]
60. Mauger, F.; Horgues, C.; Pierre-Jean, M.; Oussada, N.; Mesrob, L.; Deleuze, J.F. Comparison of commercially available whole-genome sequencing kits for variant detection in circulating cell-free DNA. *Sci. Rep.* **2020**, *10*, 6190. [CrossRef]
61. Kunadirek, P.; Chuaypen, N.; Jenjaroenpun, P.; Wongsurawat, T.; Pinjaroen, N.; Sirichindakul, P.; Nookaew, I.; Tangkijvanich, P. Cell-Free DNA Analysis by Whole-Exome Sequencing for Hepatocellular Carcinoma: A Pilot Study in Thailand. *Cancers* **2021**, *13*, 2229. [CrossRef]
62. Ma, X.; Shao, Y.; Tian, L.; Flasch, D.A.; Mulder, H.L.; Edmonson, M.N.; Liu, Y.; Chen, X.; Newman, S.; Nakitandwe, J.; et al. Analysis of error profiles in deep next-generation sequencing data. *Genome Biol.* **2019**, *20*, 50. [CrossRef] [PubMed]
63. Vijg, J. Somatic mutations, genome mosaicism, cancer and aging. *Curr. Opin. Genet. Dev.* **2014**, *26*, 141–149. [CrossRef] [PubMed]
64. Wang, Y.; Springer, S.; Mulvey, C.L.; Silliman, N.; Schaefer, J.; Sausen, M.; James, N.; Rettig, E.M.; Guo, T.; Pickering, C.R.; et al. Detection of somatic mutations and HPV in the saliva and plasma of patients with head and neck squamous cell carcinomas. *Sci. Transl. Med.* **2015**, *7*, 293ra104. [CrossRef] [PubMed]
65. Galot, R.; van Marcke, C.; Helaers, R.; Mendola, A.; Goebbels, R.M.; Caignet, X.; Ambroise, J.; Wittouck, K.; Vikkula, M.; Limaye, N.; et al. Liquid biopsy for mutational profiling of locoregional recurrent and/or metastatic head and neck squamous cell carcinoma. *Oral Oncol.* **2020**, *104*, 104631. [CrossRef]
66. Ellrott, K.; Bailey, M.H.; Saksena, G.; Covington, K.R.; Kandoth, C.; Stewart, C.; Hess, J.; Ma, S.; Chiotti, K.E.; McLellan, M.; et al. Scalable Open Science Approach for Mutation Calling of Tumor Exomes Using Multiple Genomic Pipelines. *Cell Syst.* **2018**, *6*, 271–281.e7. [CrossRef]
67. Karimnezhad, A.; Palidwor, G.A.; Thavorn, K.; Stewart, D.J.; Campbell, P.A.; Lo, B.; Perkins, T.J. Accuracy and reproducibility of somatic point mutation calling in clinical-type targeted sequencing data. *BMC Med. Genom.* **2020**, *13*, 156. [CrossRef]
68. Venning, F.A.; Wullkopf, L.; Erler, J.T. Targeting ECM Disrupts Cancer Progression. *Front. Oncol.* **2015**, *5*, 224. [CrossRef]
69. D'Aniello, C.; Patriarca, E.J.; Phang, J.M.; Minchiotti, G. Proline Metabolism in Tumor Growth and Metastatic Progression. *Front. Oncol.* **2020**, *10*, 776. [CrossRef]
70. Glunde, K.; Bhujwalla, Z.M.; Ronen, S.M. Choline metabolism in malignant transformation. *Nat. Rev. Cancer* **2011**, *11*, 835–848. [CrossRef]
71. Sivanand, S.; Vander Heiden, M.G. Emerging Roles for Branched-Chain Amino Acid Metabolism in Cancer. *Cancer Cell* **2020**, *37*, 147–156. [CrossRef]
72. Burgener, J.M.; Zou, J.; Zhao, Z.; Zheng, Y.; Shen, S.Y.; Huang, S.H.; Keshavarzi, S.; Xu, W.; Liu, F.-F.; Liu, G.; et al. Tumor-Naive Multimodal Profiling of Circulating Tumor DNA in Head and Neck Squamous Cell Carcinoma. *Clin. Cancer Res.* **2021**, *27*, 4230–4244. [CrossRef]
73. Wilson, H.L.; D'Agostino, R.B., Jr.; Meegalla, N.; Petro, R.; Commander, S.; Topaloglu, U.; Zhang, W.; Porosnicu, M. The Prognostic and Therapeutic Value of the Mutational Profile of Blood and Tumor Tissue in Head and Neck Squamous Cell Carcinoma. *Oncologist* **2021**, *26*, e279–e289. [CrossRef]
74. Wu, P.; Xie, C.; Yang, L.; Liu, Y.; Zeng, J.; Li, X.; Fang, X.; Fan, Y.; Zhao, S.; Kuang, N.; et al. The genomic architectures of tumour-adjacent tissues, plasma and saliva reveal evolutionary underpinnings of relapse in head and neck squamous cell carcinoma. *Br. J. Cancer* **2021**, *125*, 854–864. [CrossRef] [PubMed]
75. Cui, Y.; Kim, H.-S.; Cho, E.S.; Han, D.; Park, J.A.; Park, J.Y.; Nam, W.; Kim, H.J.; Cha, I.-H.; Cha, Y.H. Longitudinal detection of somatic mutations in saliva and plasma for the surveillance of oral squamous cell carcinomas. *PLoS ONE* **2021**, *16*, e0256979. [CrossRef]
76. Porter, A.; Natsuhara, M.; Daniels, G.A.; Patel, S.P.; Sacco, A.G.; Bykowski, J.; Banks, K.C.; Cohen, E.E.W. Next generation sequencing of cell free circulating tumor DNA in blood samples of recurrent and metastatic head and neck cancer patients. *Transl. Cancer Res.* **2020**, *9*, 203–209. [CrossRef]
77. Angeles, A.K.; Janke, F.; Bauer, S.; Christopoulos, P.; Riediger, A.L.; Sultmann, H. Liquid Biopsies beyond Mutation Calling: Genomic and Epigenomic Features of Cell-Free DNA in Cancer. *Cancers* **2021**, *13*, 5615. [CrossRef]
78. Chao, J.; Lee, J.; Kim, K.; Kang, S.Y.; Lee, T.; Kim, K.M.; Kim, S.T.; Klempner, S.J.; Lee, H. A Pilot Study of Baseline Spatial Genomic Heterogeneity in Primary Gastric Cancers Using Multi-Region Endoscopic Sampling. *Front. Oncol.* **2020**, *10*, 225. [CrossRef] [PubMed]
79. Li, Y.; Chen, R.; Yuan, M.; Wang, D.; Fu, C.; Chen, R.; Lei, C.; Zhou, Q. One-stop molecular classification of endometrial carcinoma using comprehensive next-generation sequencing. *Int. J. Cancer* **2022**, *151*, 1969–1977. [CrossRef] [PubMed]

80. Avanzini, S.; Kurtz, D.M.; Chabon, J.J.; Moding, E.J.; Hori, S.S.; Gambhir, S.S.; Alizadeh, A.A.; Diehn, M.; Reiter, J.G. A mathematical model of ctDNA shedding predicts tumor detection size. *Sci. Adv.* **2020**, *6*, eabc4308. [CrossRef] [PubMed]
81. Vidal, J.; Casadevall, D.; Bellosillo, B.; Pericay, C.; Garcia-Carbonero, R.; Losa, F.; Layos, L.; Alonso, V.; Capdevila, J.; Gallego, J.; et al. Clinical Impact of Presurgery Circulating Tumor DNA after Total Neoadjuvant Treatment in Locally Advanced Rectal Cancer: A Biomarker Study from the GEMCAD 1402 Trial. *Clin. Cancer Res.* **2021**, *27*, 2890–2898. [CrossRef]
82. Bachet, J.B.; Bouche, O.; Taieb, J.; Dubreuil, O.; Garcia, M.L.; Meurisse, A.; Normand, C.; Gornet, J.M.; Artru, P.; Louafi, S.; et al. RAS mutation analysis in circulating tumor DNA from patients with metastatic colorectal cancer: The AGEO RASANC prospective multicenter study. *Ann. Oncol.* **2018**, *29*, 1211–1219. [CrossRef]
83. Vidal, J.; Muinelo, L.; Dalmases, A.; Jones, F.; Edelstein, D.; Iglesias, M.; Orrillo, M.; Abalo, A.; Rodriguez, C.; Brozos, E.; et al. Plasma ctDNA RAS mutation analysis for the diagnosis and treatment monitoring of metastatic colorectal cancer patients. *Ann. Oncol.* **2017**, *28*, 1325–1332. [CrossRef]
84. Yang, M.H.; Wu, M.Z.; Chiou, S.H.; Chen, P.M.; Chang, S.Y.; Liu, C.J.; Teng, S.C.; Wu, K.J. Direct regulation of TWIST by HIF-1alpha promotes metastasis. *Nat. Cell Biol.* **2008**, *10*, 295–305. [CrossRef]
85. Gundem, G.; Van Loo, P.; Kremeyer, B.; Alexandrov, L.B.; Tubio, J.M.C.; Papaemmanuil, E.; Brewer, D.S.; Kallio, H.M.L.; Hognas, G.; Annala, M.; et al. The evolutionary history of lethal metastatic prostate cancer. *Nature* **2015**, *520*, 353–357. [CrossRef] [PubMed]
86. Brastianos, P.K.; Carter, S.L.; Santagata, S.; Cahill, D.P.; Taylor-Weiner, A.; Jones, R.T.; Van Allen, E.M.; Lawrence, M.S.; Horowitz, P.M.; Cibulskis, K.; et al. Genomic Characterization of Brain Metastases Reveals Branched Evolution and Potential Therapeutic Targets. *Cancer Discov.* **2015**, *5*, 1164–1177. [CrossRef]
87. Leemans, C.R.; Snijders, P.J.F.; Brakenhoff, R.H. The molecular landscape of head and neck cancer. *Nat. Rev. Cancer* **2018**, *18*, 269–282. [CrossRef]
88. Brandwein-Gensler, M.; Smith, R.V. Prognostic indicators in head and neck oncology including the new 7th edition of the AJCC staging system. *Head Neck Pathol.* **2010**, *4*, 53–61. [CrossRef] [PubMed]
89. Cancer Genome Atlas Research Network; Weinstein, J.N.; Collisson, E.A.; Mills, G.B.; Shaw, K.R.; Ozenberger, B.A.; Ellrott, K.; Shmulevich, I.; Sander, C.; Stuart, J.M. The Cancer Genome Atlas Pan-Cancer analysis project. *Nat. Genet.* **2013**, *45*, 1113–1120.
90. Larson, D.E.; Harris, C.C.; Chen, K.; Koboldt, D.C.; Abbott, T.E.; Dooling, D.J.; Ley, T.J.; Mardis, E.R.; Wilson, R.K.; Ding, L. SomaticSniper: Identification of somatic point mutations in whole genome sequencing data. *Bioinformatics* **2012**, *28*, 311–317. [CrossRef]
91. Ewing, A.D.; Houlahan, K.E.; Hu, Y.; Ellrott, K.; Caloian, C.; Yamaguchi, T.N.; Bare, J.C.; P'ng, C.; Waggott, D.; Sabelnykova, V.Y.; et al. Combining tumor genome simulation with crowdsourcing to benchmark somatic single-nucleotide-variant detection. *Nat. Methods* **2015**, *12*, 623–630. [CrossRef] [PubMed]
92. Lai, Z.; Markovets, A.; Ahdesmaki, M.; Chapman, B.; Hofmann, O.; McEwen, R.; Johnson, J.; Dougherty, B.; Barrett, J.C.; Dry, J.R. VarDict: A novel and versatile variant caller for next-generation sequencing in cancer research. *Nucleic Acids Res.* **2016**, *44*, e108. [CrossRef]
93. Karlsson, J.; Nilsson, L.M.; Mitra, S.; Alsen, S.; Shelke, G.V.; Sah, V.R.; Forsberg, E.M.V.; Stierner, U.; All-Eriksson, C.; Einarsdottir, B.; et al. Molecular profiling of driver events in metastatic uveal melanoma. *Nat. Commun.* **2020**, *11*, 1894. [CrossRef]
94. Steensma, D.P. Clinical consequences of clonal hematopoiesis of indeterminate potential. *Blood Adv.* **2018**, *2*, 3404–3410. [CrossRef] [PubMed]
95. Lin, S.C.; Lin, L.H.; Yu, S.Y.; Kao, S.Y.; Chang, K.W.; Cheng, H.W.; Liu, C.J. FAT1 somatic mutations in head and neck carcinoma are associated with tumor progression and survival. *Carcinogenesis* **2018**, *39*, 1320–1330. [CrossRef] [PubMed]
96. Martinez-Jimenez, F.; Muinos, F.; Sentis, I.; Deu-Pons, J.; Reyes-Salazar, I.; Arnedo-Pac, C.; Mularoni, L.; Pich, O.; Bonet, J.; Kranas, H.; et al. A compendium of mutational cancer driver genes. *Nat. Rev. Cancer* **2020**, *20*, 555–572. [CrossRef] [PubMed]
97. Friedlaender, A.; Nouspikel, T.; Christinat, Y.; Ho, L.; McKee, T.; Addeo, A. Tissue-Plasma TMB Comparison and Plasma TMB Monitoring in Patients with Metastatic Non-small Cell Lung Cancer Receiving Immune Checkpoint Inhibitors. *Front. Oncol.* **2020**, *10*, 142. [CrossRef] [PubMed]
98. Gandara, D.R.; Paul, S.M.; Kowanetz, M.; Schleifman, E.; Zou, W.; Li, Y.; Rittmeyer, A.; Fehrenbacher, L.; Otto, G.; Malboeuf, C.; et al. Blood-based tumor mutational burden as a predictor of clinical benefit in non-small-cell lung cancer patients treated with atezolizumab. *Nat. Med.* **2018**, *24*, 1441–1448. [CrossRef] [PubMed]
99. Sequeira, I.; Rashid, M.; Tomas, I.M.; Williams, M.J.; Graham, T.A.; Adams, D.J.; Vigilante, A.; Watt, F.M. Genomic landscape and clonal architecture of mouse oral squamous cell carcinomas dictate tumour ecology. *Nat. Commun.* **2020**, *11*, 5671. [CrossRef]
100. Vettore, A.L.; Ramnarayanan, K.; Poore, G.; Lim, K.; Ong, C.K.; Huang, K.K.; Leong, H.S.; Chong, F.T.; Lim, T.K.; Lim, W.K.; et al. Mutational landscapes of tongue carcinoma reveal recurrent mutations in genes of therapeutic and prognostic relevance. *Genome Med.* **2015**, *7*, 98. [CrossRef]